Glass Europe Vol. 3 (2025) 89-103

https://doi.org/10.52825/glass-europe.v3i.2593

Submitted: 10 Feb. 2025 | Accepted: 17 Mar. 2025 | Published: 08 May 2025

Controlling Internal Crystallization of $Li_2Si_2O_5$ Glass-Ceramics Using SnO_2

Markus Rampf* and Marc Dittmer

Ivoclar Vivadent AG, Liechtenstein

*Correspondence: Markus Rampf, markus.rampf@ivoclar.com

Abstract. The impact of adding SnO_2 on the nucleation and crystallization of glasses within the SiO_2-Li_2O-Al_2O_3-K_2O glass system is investigated. Minor amounts of SnO_2 (0.01 mol%) yield significant differences in the crystallization sequence and microstructure of these glass-ceramics. Adding SnO_2 instigates the formation of Li_2SiO_3 as the primary crystal phase along with $Li_2Si_2O_5$ at temperatures below 600 °C. Annealing at 950 °C for 10 minutes yields glass-ceramics with $Li_2Si_2O_5$ as the sole crystalline phase. However, SnO_2 cannot be empirically deduced as having a direct role in nucleation. Further, the study explores the effect of SnO_2 concerning crystal formation, yet its exact role and effects remain somewhat ambiguous, necessitating continued investigations. Notably, the research results in a glass-ceramic with an unique microstructure comprising up to 70 wt% comparable large $Li_2Si_2O_5$ crystals yielding a fracture toughness of up to 3 $MPa*m^{1/2}$ and a biaxial fracture strength significantly above 300 MPa. These characteristics warrant exploring potential applications in areas demanding materials with a robust combination of toughness and strength, such as dental prosthetics.

Keywords: Glass-Ceramics, Lithium Disilicate, Nucleation

1. Introduction

Glass has been known and used for many centuries. By chance, $Li_2Si_2O_5$ glass-ceramics were discovered in the 1950s by D. Stookey [1]. In the following decades, the controlled devitrification of glasses applying various technologies to affect nucleation and crystal growth was used to engineer glass-ceramics for many different applications [2], [3]. The appropriate composition of the base glass, along with precise knowledge of nucleation and crystal growth are of paramount importance.

The lithium silicate system has been studied intensively since its discovery by D. Stookey. The stoichiometric Li_2O-$2SiO_2$ glass system (33.33 mol% Li_2O; 66.66 mol% SiO_2) has been investigated in terms of nucleation and crystallization. It has been shown that both, homogeneous and heterogeneous nucleation is possible in the stoichiometric system [2], [4], [5], [6], [7], [8]. The non-stoichiometric system and multicomponent compositions have also been intensively studied. It was shown early on that phase separation occurs in non-stoichiometric systems [9]. Additives can alter the mechanism of nucleation and crystallization. For example, Na_2O up to 11 mol% leads to homogeneous nucleation, while higher levels promote surface crystallization [10]. Additives such as Al_2O_3 and K_2O can improve chemical durability [11]. Colloidal silver particles [1], [12] and P_2O_5 [13] can be used as nucleating agents to achieve heterogeneous nucleation [2], [14]. Other additives such as Cs_2O, Nb_2O_5, Ta_2O_5 or divalent oxides like MgO and/or CaO can be used to precipitate secondary phases such as $Ca_5(PO_4)_3F$, $CsAlSi_5O_{12}$, quartz, niobates or tantalates [15], [16], [17], [18], [19].

As early as the 1970s and 1980s, it was shown that very good mechanical properties were possible for a glass ceramic with a flexural strength between 100 and 300 MPa and a fracture toughness between 2 and 3 MPa*$m^{1/2}$ [20], [21], [22]. In the following decades, the mechanical properties were further improved by changing the residual glass phase and adjusting the microstructure. It was possible to produce translucent glass-ceramics with a flexural strength between 150 and 250 MPa and a fracture toughness of about 3 MPa*$m^{1/2}$ with a crystal phase content of about 80 wt%. These high mechanical properties were made possible by a special interlocking microstructure in which a crack is deflected by the corresponding structure [23] [24]. By further adjusting the glass composition and the respective nucleation and crystallization temperatures, flexural strength of up to 740 MPa could be achieved for samples produced in the laboratory [25], [26]. P_2O_5 so far proofed to be the most efficient agent for internal nucleation which enabled a high crystalline ratio of 60 vol% $Li_2Si_2O_5$ arranged in an interlocking manner. In order to understand the mechanism of this nucleating agent, fundamental investigations were carried out using DSC measurements, high-temperature XRD measurements, high-resolution SEM analyses and NMR measurements. These showed that amorphous or nanocrystalline disordered Li_3PO_4 separates in form of a glass-glass phase separation prior to nucleation and crystal growth. The high energy interface of this glass in glass phase separation was discussed to nucleate lithium silicate crystals. Li_2SiO_3 then crystallizes at lower crystallization temperatures, dissolves again at higher crystallization temperatures and in parallel the crystallization rate of $Li_2Si_2O_5$ increases sharply [2].

To increase the strength of glass-ceramics, different approaches have been chosen in the past and, as already mentioned, successfully implemented. High strengths can be achieved through high crystal phase contents, fine interlocked microstructures, as well as by subsequent treatment such as the induction of thermal stresses or ion exchange processes [2]. To increase the toughness, several approaches are already known and have been investigated [27], [28]. However, a significant increase in toughness, of the same magnitude as has been achieved with strength, is much more challenging. Mechanisms based on the microstructure design, such as crack deflection and microcrack formation, have so far shown the greatest success [27], while residual stress effects [28] or phase transformation mechanisms (as used in ZrO_2 ceramics) have so far only been presented conceptually or, if at all, have only been empirically proven on model systems at the microscale. Given the state of the art for $Li_2Si_2O_5$ glass ceramics, a material with the highest possible content of large interlocking crystals in the structure promises the most promising toughness properties. In order to achieve this, highly efficient nucleation and conversion of the base glass components into $Li_2Si_2O_5$ is required. The use of P_2O_5 as a nucleating agent presents a challenge in this context due to its limited efficiency and significant binding of Li^+ in the form of Li_3PO_4 (crystalline and amorphous), which thus is not available for the formation of $Li_2Si_2O_5$ [19], [29].

In the present work a successful approach to produce high toughness $Li_2Si_2O_5$ glass-ceramics via internal nucleation without using P_2O_5 is investigated. The addition of SnO_2 proofed to enable efficient internal nucleation and crystallization of $Li_2Si_2O_5$. The underlying mechanism and processes, however, are still unclear. A few hints about the function of SnO_2 can be found in the literature. Ehrt et al. [30], [31] studied the redox behavior of SnO_2 used in glass. They showed that there is a ratio of Sn^{2+} to Sn^{4+} that depends on the melting temperature. Sn^{4+} was the favored state in silicate glasses under oxidizing or reducing melting conditions between 1600 and 1700°C. They found only 1 to 2 % of Sn^{2+} in these glasses. Doenitz et al. described the segregation-promoting effect of SnO_2 [32] and investigated its effect on the crystallization of a magnesium aluminosilicate glass. However, it turned out that SnO_2 had only a minor effect on volume crystallization, which was then dominated by surface crystallization processes. Zhang et al. studied glasses in the Lithium-Alumosilicate composition range with additions of ZrO_2 and SnO_2 to form β-quartz-solid-solution [33]. They found that SnO_2 alone had no effect on crystallization of β-quartz-solid-solution. Dressler et al. investigated the crystallization behavior of lithium alumosilicate glass-ceramics with additions of ZrO_2 and SnO_2, where the nucleation rate increased with increasing SnO_2 content, but the crystal growth rate hardly increased at all [34]. Thieme et al. discussed a nucleating effect of SnO_2 in the

$BaO-SrO-ZnO-SiO_2$ glass system. They found metallic Sn and Pt clusters in the center of the crystals. The latter diffuses from the crucible material into the melt. Ultimately, they left the question open as to whether only the combination of Pt and Sn would produce a nucleating effect [35]. Ziemath et al. investigated additions of SnO_2 in silicate glasses. They found SnO_2 to increase the glass transition temperature, density and hardness of the glasses and therefore suggested a network forming role of SnO_2 [36] while in contrast Zhao et al. reported small amounts of SnO_2 to act as a network modifier and to increase the tendency for a glass to crystallize [37].

2. Experimental Procedure

2.1 Glass formation and thermal analysis

Glasses of the system SiO_2-Li_2O-Al_2O_3-K_2O with SnO_2 with a fixed molar ratio of SiO_2/Li_2O of 2.4 were melted from the raw materials quartz, lithium carbonate, aluminium oxyhydroxyhydrate, potassium carbonate and tin dioxide in batches of 100 to 200 g in an uncovered Pt-Rh10 crucible. The compositions are given in Table 1.

***Table 1**. Calculated composition of the parent glasses in mol%.*

Composition	SiO_2 (mol%)	Li_2O (mol%)	K_2O (mol%)	Al_2O_3 (mol%)	SnO_2 (mol%)
Ref	69.20	28.80	1.00	1.00	0
Sn-0.01	69.18	28.81	1.00	1.00	0.01
Sn-0.4	68.90	28.70	1.00	1.00	0.40
Sn-0.75	68.88	28.59	1.00	1.00	0.75
Sn-1.0	68.50	28.50	1.00	1.00	1.00

After one hour at 1650 °C, the melts were poured into water, crushed and dried at 150 °C for about one hour. Thermal analyses were carried out by differential scanning calorimetry (DSC) in a nitrogen atmosphere at a heating rate of 10 K/min up to 1200 °C (STA 449 Jupiter F3, Netzsch, Selb, Germany). The frits were remelted at 1650 °C for one hour. Blocks measuring 13 mm × 13 mm × 30 mm were cast in a graphite mould and then placed in a furnace preheated to 480 °C. After a holding time of 10 minutes, the furnace was turned off and cooled to room temperature at a rate of about 2 to 3 K/min. This cooling was necessary to relieve stresses in the glass blocks and allow further mechanical processing of the glass blocks, while the holding time was used to generate nuclei for crystallization. The temperature was chosen based on the T_g determined for the various base glasses, assuming that any crystal growth below a temperature of T_g + 20 K would be negligible in this glass system.

2.2 Crystallization, X-ray diffraction and Rietveld-refinement

To characterize the crystal phases, small plates of 13 mm × 14 mm × 2 mm were cut from glass blocks and crystallized in a Programat® furnace (Ivoclar Vivadent AG, Schaan, Liechtenstein) with different annealing schedules. The samples were annealed at 570, 600, 700, 800, 900 and 950 °C for 10 min.

After annealing, the surfaces of the samples were ground with a 125 µm diamond disc. XRD patterns were recorded from the ground samples with $Cu_{K\alpha}$ radiation ($\lambda = 0.154$ nm) from 10° to 60° 2θ with a step size of 0.014° using a D8-Advance diffractometer (Bruker, Karlsruhe, Germany). The PDF entries 04-005-4718 (low-quartz), 04-010-3965 ($Li_2Si_2O_5$) and 00-029-0828 (Li_2SiO_3) were used for phase identification. In addition, a quantitative study of the crystal phases was performed on selected samples using Rietveld refinement. For this purpose, selected glass-ceramics were crushed and ground in a mortar grinder (Mortar Grinder RM 200, Retsch, Haan, Germany) and then sieved < 45 µm. The ground samples were then mixed with approximately 20 wt% α-Al_2O_3 (Alfa Aesar, 99.9 %, 20-50 µm // ICSD number: 51687) as an internal standard and eluted with acetone. After drying these mixtures in an oven preheated to 80 °C, XRD patterns were recorded from 10° to 100° 2θ in 0.014° steps. Quantification of the crystal phases was performed using Bruker's TOPAS software.

2.3 Mechanical properties

The biaxial fracture strength σ_{biax} was determined according to ISO 6872, including surface finishing with a 15 µm diamond grinding disk. The specimens were milled from glass blocks using a CEREC® InLab milling machine (Sirona, Bensheim, Germany). The measurements were conducted using a universal testing apparatus (Zwick 1456, Zwick GmbH & Co. KG, Ulm, Germany). Biaxial strengths are reported as the mean of ten to twelve data sets ± standard deviation.

The fracture toughness K_{Ic} of the glass ceramics was determined by means of SEVNB method according to ISO 6872. Bars of the approximate test size were cut from the glass blocks, crystallized and ground to the required dimensions using a 40 µm diamond grit grinding disk. Subsequently, the notch was prepared using a razor blade.

2.4 Microstructure

The microstructures of the glass ceramics crystallized at different temperatures were examined by scanning electron microscopy (SEM). The surface of the glass plates was treated with a 0.5 µm diamond grinding disk, and then etched in 3 % HF acid for 10 s. Prior to SEM analysis, the samples were coated with a 1-2 nm thick AuPd layer. The SEM examinations were performed with a Supra 40VP (Carl Zeiss, Oberkochen, Germany) electron microscope.

3. Results

3.1 Glass formation and thermal analysis

All the glasses obtained were transparent. The results of the thermal analysis are shown in Figure 1 and Table 2. The glass transition temperature T_g of all glasses is the same within the error limits. The reference sample shows an exothermic peak at 689 °C. All compositions with Sn show another exothermic peak between 870 and 883 °C. In addition, the Sn-0.4 and Sn-0.75 compositions show another small peak between 635 and 652 °C. The dissolution or melting of the crystalline phases can be seen in the endothermic peak T_{endo}, with the compositions Ref, Sn-0.01 and Sn-0.4 having a similar temperature. A further increase in SnO_2 content leads to a reduction in T_{endo} to 1008 °C.

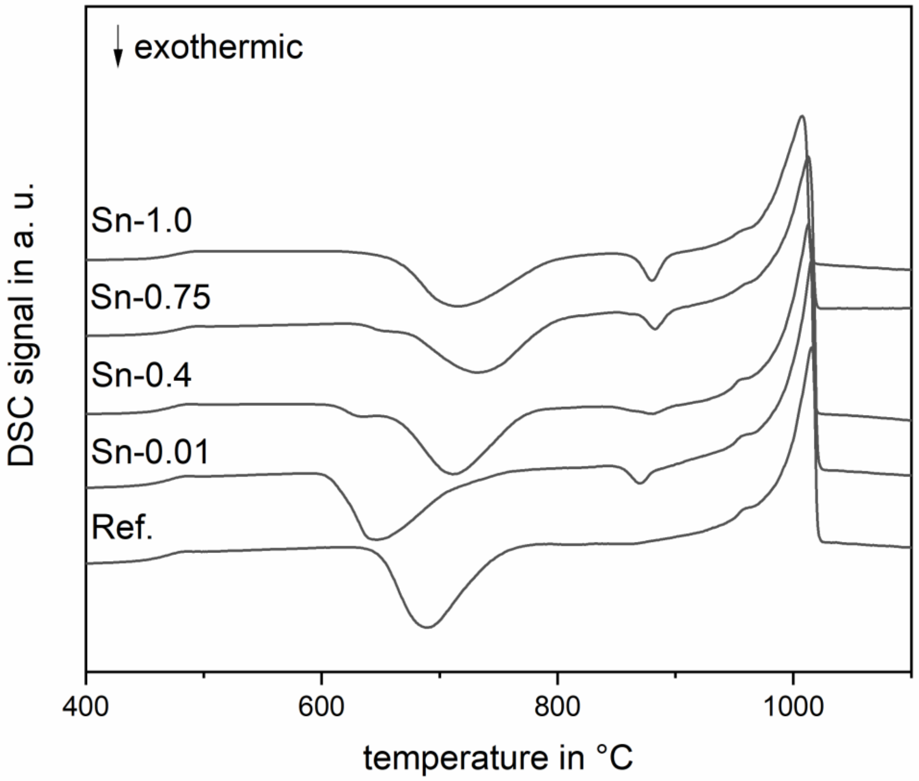

Figure 1. *Thermal analysis of the parent glasses by means of DSC.*

Table 2. *Glass transition temperature (T_g) and peak temperatures of exothermic (T_{exo1}, T_{exo2}, T_{exo3}) and endothermic (T_{endo1}) signals as determined by DSC.*

Characteristic Temperature (°C)	**Ref**	**Sn-0.01**	**Sn-0.4**	**Sn-0.75**	**Sn-1.0**
T_g	463	462	463	463	461
T_{exo1}	689	647	637	652	-
T_{exo2}	-	-	713	730	716
T_{exo3}	-	871	883	881	881
T_{endo1}	1015	1017	1014	1011	1008

3.2 Qualitative and quantitative phase analysis

Figure 2 shows the XRD patterns of all samples annealed at 600 °C for 10 min. The reference sample Ref showed no crystalline phase, while Li_2SiO_3 and $Li_2Si_2O_5$ were obtained in the SnO_2 comprising samples.

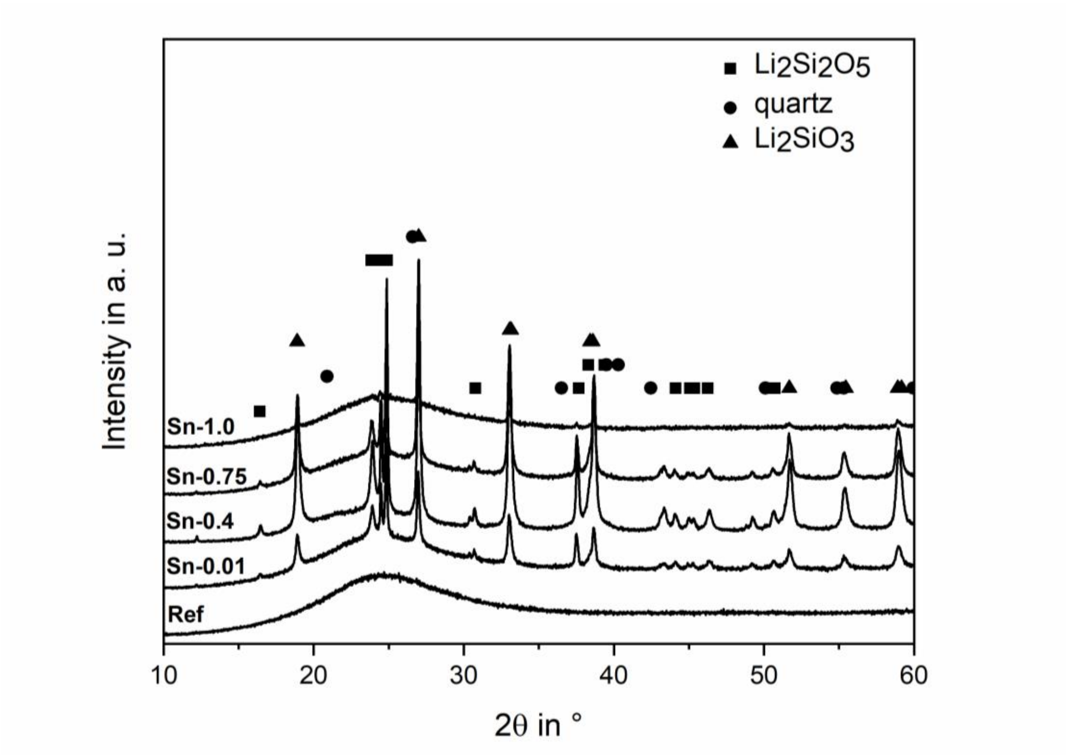

Figure 2. *Diffractograms of glass-ceramics annealed at 600 °C for 10 min.*

Figure 3 shows the diffractograms of the glass-ceramics after crystallization at 800 °C for 10 min. The reference sample shows $Li_2Si_2O_5$ as the only crystalline phase, while both $Li_2Si_2O_5$ and Li_2SiO_3 can be found in the other samples. After crystallization at 950 °C for 10 min $Li_2Si_2O_5$ is the main crystalline phase with minor concentrations of quartz and Li_2SiO_3 in samples Sn-0.01 and Sn-1.0 present as shown in Figure 4.

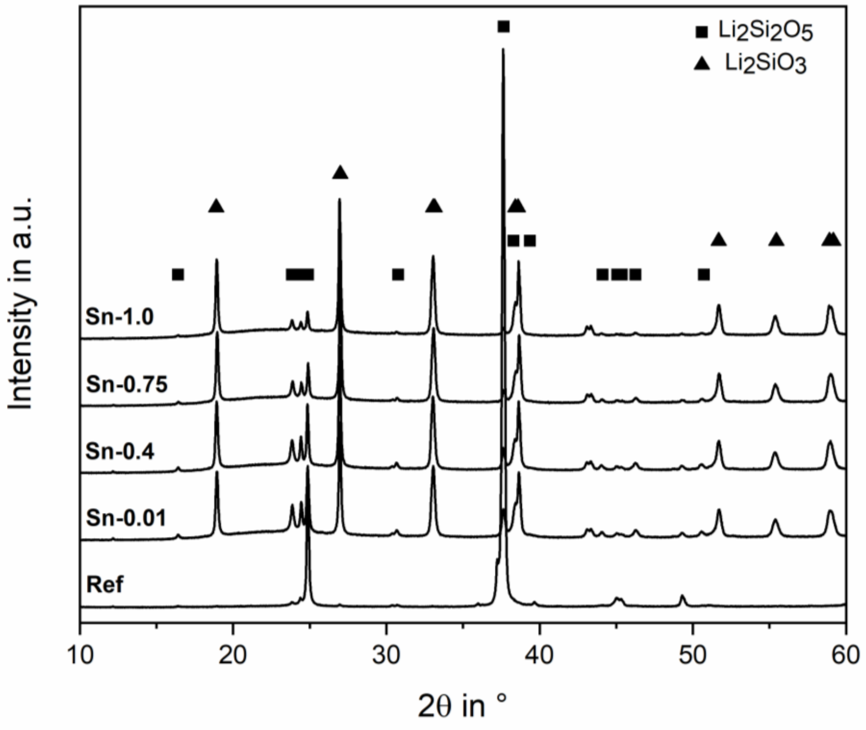

Figure 3. *Diffractograms of glass-ceramics annealed at 800 °C for 10 min.*

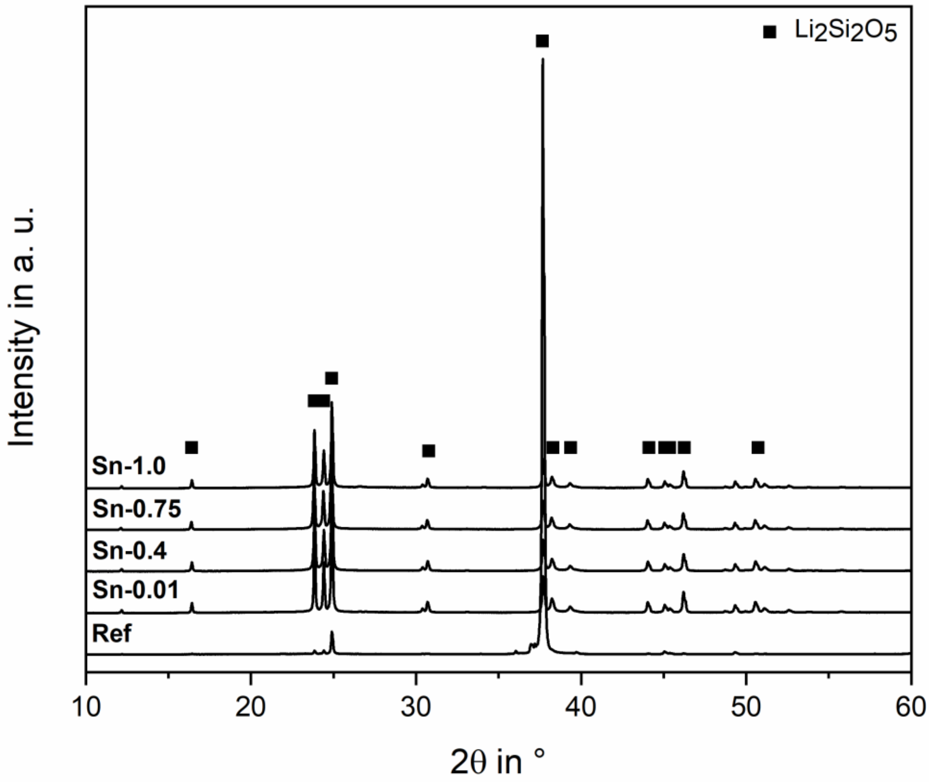

Figure 4. *Diffractograms of glass-ceramics annealed at 950 °C for 10 min.*

The diffraction patterns of the reference sample free from SnO_2 and the diffractograms of all SnO_2 containing samples heat treated at 800 °C or 950 °C for 10 minutes differ significantly. Notably, there is a strong emphasis on individual $Li_2Si_2O_5$ reflection peaks in the reference sample. This results in a significant deviation of the intensity ratios of the peaks to each other compared to the theoretically expected values. This disproportionate reflection of individual lattice planes can clearly be attributed to an orientation of crystals in the microstructure.

Table 3 shows the results of the Rietveld refinement. $Li_2Si_2O_5$ is the only crystalline phase in the reference sample with about 63 to 66 wt%. For all SnO_2 comprising samples Li_2SiO_3 as the main crystalline phase and $Li_2Si_2O_5$ as minor phase can be detected and quantified already after a heat treatment at 600 °C for 10 min. Only after annealing at 950 °C for 10 min does this situation change and $Li_2Si_2O_5$ forms the main crystal phase while Li_2SiO_3 has almost completely disappeared from all samples. Very minor amounts of quartz and Li_2SiO_3 can still be found in 0.01 mol% and 1.0 mol% SnO_2 comprising glass-ceramics.

***Table 3**. Phase quantification of the glass-ceramics my means of Rietveld refinement in wt%.*

Sample	Temperature	Li_2SiO_3 (wt%)	$Li_2Si_2O_5$ (wt%)	Quartz (wt%)
Ref	800	0	63.9	0
Ref	950	0	66.2	0
Sn-0.01	600	37.0	20.0	0
Sn-0.01	800	42.1	12.4	0.3
Sn-0.01	950	0.5	71.5	0.1
Sn-0.4	600	36.4	17.7	0
Sn-0.4	800	36.9	15.9	0
Sn-0.4	950	0	69.7	0
Sn-0.75	600	29.9	9.2	0
Sn-0.75	800	42.2	9.4	0
Sn-0.75	950	0	69.7	0
Sn-1.0	600	20.0	4.3	0
Sn-1.0	800	43.5	4.3	0
Sn-1.0	950	1.5	69.0	0.9

3.3 Microstructure formation

Figure 5 shows the scanning electron micrographs of the glass-ceramics crystallized at 600 °C, 800 °C or 950 °C. The reference sample Ref shows no crystalline phase at 600 °C, whereas very large crystals can be seen at both 800 °C and 950 °C. Some of these are oriented in larger domains. In contrast, all compositions containing SnO_2 show dendritic crystals in varying numbers and sizes at both 600 and 800 °C. Large crystals are visible at 950 °C. At 950 °C, large crystals can be seen with no orientation at all.

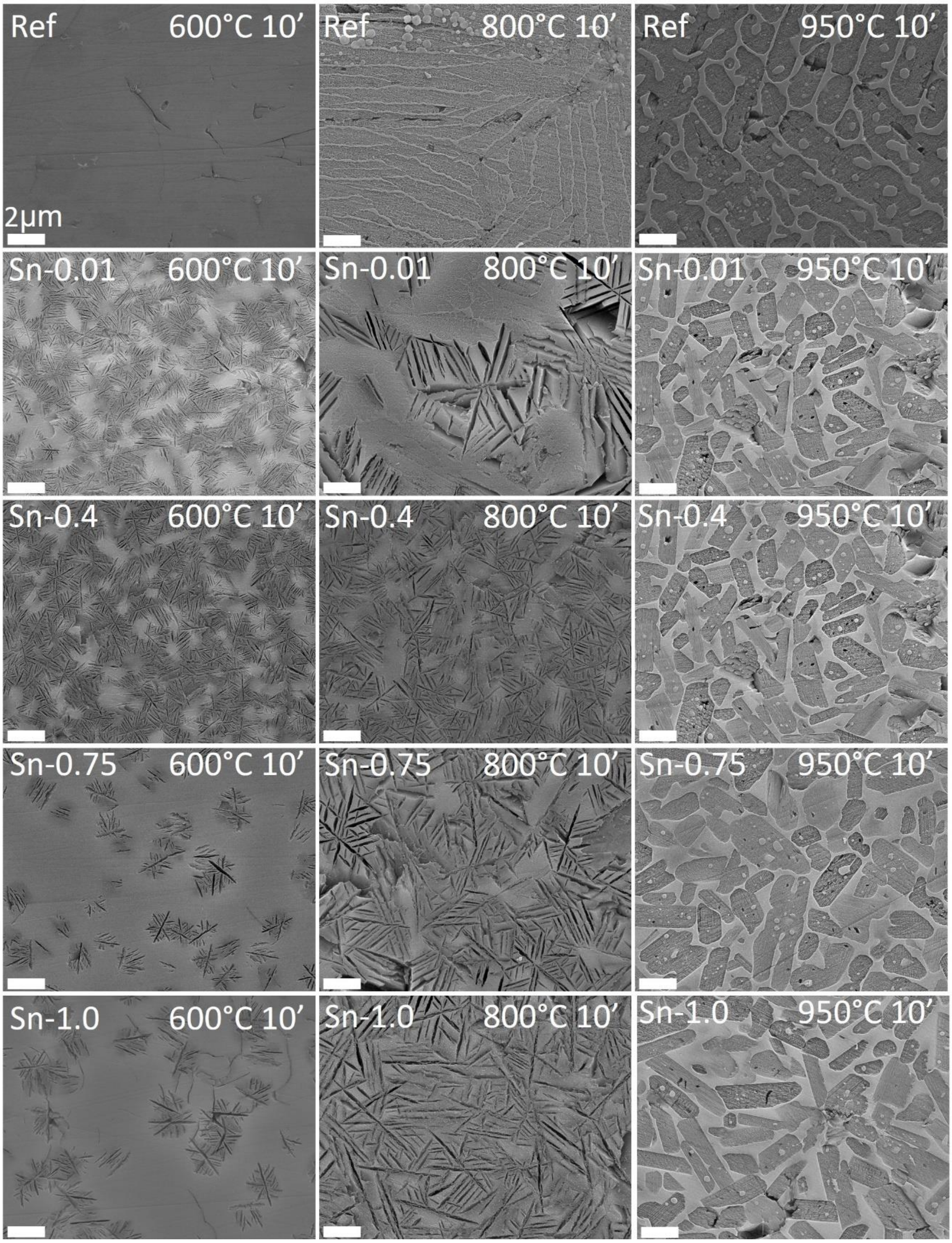

Figure 5. *Scanning electron micrographs of samples annealed at 600°C, 800°C or 950°C for 10 min.*

3.4 Mechanical properties

In table 4 the biaxial bending strength and the fracture toughness of the glass-ceramics crystallized at 950 °C for 10 min are summarized. The mechanical properties of the reference glass-ceramics could not be determined. This samples broke into several pieces during crystallization or subsequent processing due to extensive crack formation and porosity. The mean biaxial fracture strengths of the SnO_2-containing glass-ceramics Sn-0.01 (358 MPa), -0.4 (408 MPa) and -0.75 (388 MPa) are the same within the standard deviation. Only the sample with 1 mol% SnO_2 shows a significant lower biaxial strength with a mean value of 335 MPa. No significant difference in the fracture toughness could be detected for the samples Sn-0.01 (2.9 $MPa*m^{1/2}$), -0.4 (2.9 $MPa*m^{0.5}$), -0.75 (2.7 $MPa*m^{0.5}$) and -1.0 (2.9 $MPa*m^{0.5}$).

***Table 4**. Biaxial fracture strength σ_{biax} and fracture toughness K_{Ic} of samples crystallized at 950 °C for 10 min.*

Sample	σ_{biax} (MPa)	K_{Ic} ($MPa*m^{1/2}$)
Sn-0.01	358 ± 33	2.9 ± 0.2
Sn-0.4	408 ± 43	2.9 ± 0.1
Sn-0.75	388 ± 37	2.7 ± 0.1
Sn-1.0	335 ± 39	2.9 ± 0.1

4. Discussion

4.1 Nucleation and Crystal phase formation

Nucleation was not specifically investigated in this study. Therefore, only a limited phenomenological discussion based on the results of thermal glass analysis, the crystallization sequence and microstructure formation are possible in this regard. Noteworthy in the results of the thermal analysis of the parent glasses is that the addition of 0.01 mol% SnO_2 significantly reduces the temperature of the first exothermic peak compared to the reference, and thus nucleation and crystallization begin at significantly lower temperatures (Figure 1, Table 2). Surprisingly, however, increasing the SnO_2 content to 0.4 mol% shifts the temperature of the first exothermic peak to significantly higher temperatures than the reference sample. This trend continues with further increases in SnO_2 content up to 1 mol% and is also reflected in the microstructure formation (Figure 2). The microstructure comprising a high number of rather dendritic Li_2SiO_3 crystals, that is achieved with the 0.01 mol% and 0.4 mol% SnO_2 containing samples at 600 °C, can only be achieved at > 600 °C with the 0.75 mol% and 1.0 mol% SnO_2 containing glasses (Figure 6). In all cases, the addition of SnO_2, regardless of the concentration compared to the reference, leads to a second exothermic peak at temperatures above 850 °C (Figure 1, Table 2). Considering the results from the phase analysis (Figure 4, Table 3), this peak is attributed to the enhanced crystallization of $Li_2Si_2O_5$. To summarize, these results establish that the addition of SnO_2, depending on the concentration, has fundamentally different effects that could not be separated or decoded in detail. The increased tendency for crystallization of the SnO_2 comprising glasses could indicate the role as a network modifier, as described by Zhao et. al [37]. In this context, the influence of SnO_2 on nanoscale composition fluctuations could also be considered for future investigations and discussions [8]. The promotion of early crystallization of Li_2SiO_3 could, in this regard, also indicate the facilitation of the formation of Li_2O-rich regions where Li_2SiO_3 is prone to nucleate.

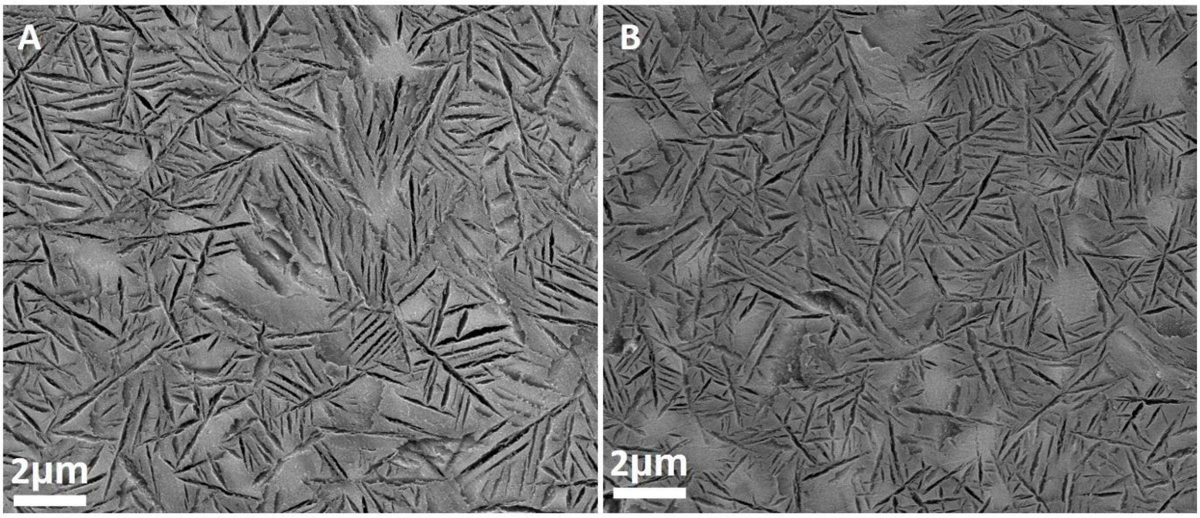

Figure 6. *Micrographs of sample A) Sn-0.75 and B) Sn-1.0 after crystallization at 700 °C for 10 min.*

A direct role of SnO_2 in the nucleation of lithium silicates, for example through epitaxy or the formation of a phase boundary, is rather unlikely. On the one hand, these mechanisms could hardly be explained with the extremely low amounts of SnO_2 that were found to be effective here, and on the other hand, an influence of the amount of nucleating agent used on the microstructure itself would have to be observed. If a direct mechanism is present, it is to be assumed that an increase in the nucleating agent concentration should lead to a larger number of crystallization nuclei and thus to a finer microstructure. Although the melting point of SnO_2, at approximately 1630 °C, is just below the temperature at which the mixtures were melted, it can be assumed that SnO_2 was completely dissolved in the glass. All glasses produced were X-ray amorphous. Even the glass made from the mixture with 1 mol% SnO_2 showed no residual crystalline phase.

Metal clusters were reported to act as highly efficient agents to catalyze nucleation and crystallization [1], [12], [13]. These typically work already in quantities < 0.1 mol% as it is the case in the present work. The probability of forming clusters of metallic Sn is not clear. The raw material batches did not contain a specific reducing agent. Thus, a reduction of SnO_2 to metallic Sn purely through a reducing atmosphere at the high temperatures during the melting process is conceivable. Even in this case, however, one would have to assume an influence of the nucleating agent concentration on the microstructure formation, which could not be demonstrated experimentally. The very limited possibilities for reducing SnO_2 in the present experimental setup could however also provide an explanation for why an increase in the SnO_2 content does not lead to more metallic Sn clusters and thus more crystal nuclei being formed. Identifying the very function of SnO_2 on nucleation and crystallization as well as the underlying mechanisms require further dedicated research.

Introducing even very small amounts of SnO_2 significantly changes the crystallization. The effect is evident in the thermal analysis of the glass (Figure 1, Table 2), the phase sequence of crystallization (Table 3), and the microstructure of the glass-ceramics (Figure 5). While the reference sample Ref shows only $Li_2Si_2O_5$ as detectable crystalline phase after annealing above 800 °C, the addition of 0.01 mol% SnO_2 already leads to the formation of Li_2SiO_3 and $Li_2Si_2O_5$ at a crystallization temperature < 600 °C. Li_2SiO_3 forms the main crystal phase. Interestingly, the proportion of both $Li_2Si_2O_5$ as well as Li_2SiO_3 decreases significantly at this crystallization temperature with an increase in the SnO_2 content in the composition. For the SnO_2-containing compositions, regardless of the concentration, Li_2SiO_3 remains the main crystal phase for temperatures < 900 °C. Only after a temperature treatment > 800 °C, the proportion of Li_2SiO_3 and residual glass decreases at the expense of $Li_2Si_2O_5$ until the latter phase forms the main crystal phase. This sequence of crystallization has typically been reported for lithium silicate glass systems when P_2O_5 was used as nucleating agent [2]

4.2 Microstructure formation and mechanical properties

The significantly different crystallization of the reference sample compared to the SnO_2-containing samples is also evident in the micrographs in Figure 5. The addition of SnO_2 was able to prevent the formation of highly oriented $Li_2Si_2O_5$ clusters and enabled the formation of a homogeneous structure with isotropic properties. The large, oriented crystals in the reference samples clearly indicate inefficient volume nucleation. The microstructure could be the result of random homogeneous nucleation. The formation of large oriented $Li_2Si_2O_5$ crystals leads to large local density differences and thus will hinder the formation of a dense and mechanically stable solid. This could explain why all the reference samples disintegrated during crystallization and it was not possible to prepare solid body samples for mechanical analyses.

The very reproducibly high fracture toughness can be attributed to the structure consisting of comparatively large $Li_2Si_2O_5$ crystals [28]. The dominant mechanism here is most likely to be crack deflection [27], [28]. Although coarse structures usually achieve relatively low strength values, in this case strengths well above 350 MPa could be reliably achieved. This can be attributed primarily to the high content of crystalline phase.

The combination of very high toughness and good strength is almost unique for glass-ceramic materials and is of interest, for example, for use in dental prosthetics.

5. Conclusion

The addition of even the smallest amounts of SnO_2 significantly changes the nucleation and crystallization of glasses in the SiO_2-Li_2O-Al_2O_3-K_2O system. Without SnO_2, only $Li_2Si_2O_5$ crystallizes in the form of very large and oriented crystalline domains at temperatures > 700 °C. The resulting large local differences in density lead to high stresses and result in cracks followed by disintegration that prevent the production of a homogeneous dense solid. Adding SnO_2 leads to the formation of Li_2SiO_3 as the main crystal phase along with $Li_2Si_2O_5$ at temperatures < 600 °C. From crystal growth temperatures >800 °C, all Li_2SiO_3 converts into $Li_2Si_2O_5$. This phase sequence allows the production of solid bodies with a homogeneous structure of large interlocking $Li_2Si_2O_5$ crystals. In contrast to the use of P_2O_5 as a nucleating agent, no Li^+ is bound in the form of amorphous or (disordered nano-)crystalline Li_3PO_4 and is completely available for the formation of $Li_2Si_2O_5$. The thus achieved high crystalline phase contents of approx. 70 wt% enable a glass-ceramic material with a very advantageous combination of comparable very high toughness and high fracture strength.

A direct role of SnO_2 in the nucleation mechanism can phenomenologically be ruled out. Whether SnO_2 is involved in nucleation or solely effects crystal growth is not clear. Furthermore, the exact role of SnO_2 is supposed to be depended on its concentration in the parent glass, however, could not be identified in detail and requires further dedicated investigations.

Data availability statement

Data will be made available on request.

Author contributions

Markus Rampf and Marc Dittmer: Conceptualization, Investigation, Methodology, Validation, Writing – review & editing.

Competing interests

The authors declare that they have no competing interests.

References

[1] S.D. Stookey, “Catalyzed crystallization of glass in theory and practice”, Ind. Eng. Chem., vol. 51 no. 7, pp. 805-808, July 1959, doi: https://doi.org/10.1021/ie50595a022.

[2] W. Höland, G. H. Beall, “Alkaline and Alkaline Earth Silicates-SiO_2-Li_2O (Lithium Disilicate)” in Glass-Ceramic Technology 3rd ed., Hoboken, New Jersey: Wiley, 2020, ch. 2.1, sec. 2.1.1, pp. 67-78.

[3] J. Deubener, M. Allix, M.J. Davis, A. Duran, T. Höche, T. Honma, T. Komatsu, S. Krüger, I. Mitra, R. Müller, S. Nakane, M.J. Pascual, J.W.P. Schmelzer, E.D. Zanotto, S. Zhou, “Updated definition of glass-ceramics”, J. Non-Cryst. Solids, vol. 501, pp. 3-10, December 2018, doi: https://doi.org/10.1016/j.jnoncrysol.2018.01.033.

[4] E.M. Levin, C.R. Robbins, H.F. McMurdie, “Phase Diagrams for Ceramists”, 3rd volume, Columbus, Ohio: The American Ceramic Society, 1964.

[5] C. Rüssel, R. Keding, “A new explanation of the induction period observed during nucleation of lithium disilicate glass”, J. Non-Cryst. Solids, vol. 328 no. 1-3, pp. 174-182, October 2003, doi: https://doi.org/10.1016/S0022-3093(03)00468-X.

[6] J. Deubener, R. Brückner, M. Sternitzke, “Induction time analysis of nucleation and crystal growth in di- and metasilicate glasses”, J. Non-Cryst. Solids, vol. 163 no. 1, pp. 1-12, October 1993, doi: https://doi.org/10.1016/0022-3093(93)90638-E.

[7] J. Deubener, “Structural aspects of volume nucleation in silicate glasses”, J. Non-Cryst. Solids, vol. 351 no. 18, pp. 1500-1511, June 2005, doi: https://doi.org/10.1016/j.jnoncrysol.2004.04.028.

[8] T. Komatsu, T. Honma, “Nanoscale composition fluctuations and crystallization process: Case study in Li_2O–SiO_2-based glasses”, Int. J. Appl. Glass Sci., vol. 13 no. 4, pp. 591-609, October 2022, doi: https://doi.org/10.1111/ijag.16583.

[9] W. Vogel, "Struktur und Kristallisation der Gläser", Leipzig, Dt. Verlag für Grundstoffindustrie, 1963.

[10] J. Deubener, “Compositional onset of homogeneous nucleation in (Li, Na) disilicate glasses”, J. Non-Cryst. Solids, vol. 274 no. 1-3, pp. 195-201, September 2000, doi: https://doi.org/10.1016/S0022-3093(00)00188-5.

[11] W. Freiman, L.L. Hench, “Effect of crystallization on the mechanical properties of Li_2O-SiO_2 glass-ceramics”, J. Amer. Ceram. Soc., vol 55 no. 2, pp. 86-90, February 1972, doi: https://doi.org/10.1111/j.1151-2916.1972.tb11216.x.

[12] G.H. Beall, “Design and properties of glass-ceramics”, Annu. Rev. Mater. Sci., vol. 22, pp. 91-119, August 1992, doi: https://doi.org/10.1146/annurev.ms.22.080192.000515.

[13] T.J. Headley, R.E. Loehman, “Crystallization of a glass-ceramics by epitaxial growth”, J. Amer. Ceram. Soc., vol. 67 no. 9, pp. 620-625, September 1984, doi: https://doi.org/10.1111/j.1151-2916.1984.tb19606.x.

[14] A. V. DeCeanne, L. R. Rodrigues, C. J. Wilkinson, J. C. Mauro, E. D. Zanotto, “Examining the role of nucleating agents within glass-ceramic systems”, J. Non-Cryst. Solids, vol. 591, September 2022, doi: https://doi.org/10.1016/j.jnoncrysol.2022.121714.

[15] M. Rampf, M. Dittmer, C. Ritzberger, M. Schweiger, W. Höland, “Properties and crystallization phenomena in $Li_2Si_2O_5$–$Ca_5(PO_4)_3F$ and $Li_2Si_2O_5$–$Sr_5(PO_4)_3F$ glass–ceramics via twofold internal crystallization”, Front. Bioeng. Biotechnol., 3;3:122, September 2015, doi: 10.3389/fbioe.2015.00122. PMID: 26389112; PMCID: PMC4558524.

[16] M. Rampf, M. Fisch, M. Dittmer, C. Ritzberger, W. Höland, “Tailoring the thermal expansion of glass-ceramics by controlled twofold crystallization of $Li_2Si_2O_5$ and $CsAlSi_5O_{12}$”, Int. J. of Appl. Glass-Sci., vol. 7 no. 3, pp. 285-294, December 2015, doi: https://doi.org/10.1111/ijag.12180.

[17] M. Rampf, M. Dittmer, C. Ritzberger, W. Höland, “Controlled Parallel Crystallization of Lithium Disilicate and Diopside Using a Combination of Internal and Surface Nucleation”, Front. Mater., vol. 3, October 2016, doi: https://doi.org/10.3389/fmats.2016.00047.

[18] M. Dittmer, C. Ritzberger, W. Höland, M. Rampf, “Controlled precipitation of lithium disilicate ($Li_2Si_2O_5$) and lithium niobate ($LiNbO_3$) or lithium tantalate ($LiTaO_3$) in glass-ceramics”, J. Europ. Cer. Soc., vol. 38 no. 1, pp. 263-269, January 2018, doi https://doi.org/10.1016/j.jeurceramsoc.2017.08.032.

[19] M. Rampf, M. Fisch, G. Helsch, J. Deubener, C. Ritzberger, W. Höland, M. Dittmer, “Quartz-containing glass-ceramics in the SiO_2–Li_2O–K_2O–MgO–CaO–Al_2O_3–P_2O_5 system”, Applied Glass Science, vol. 10 no. 3, pp. 330-338, July 2019, doi: https://doi.org/10.1111/ijag.13095.

[20] P. Hing, P.W. McMillan, “The strength and fracture properties of glass-ceramics”, J. Mater. Sci., vol. 8, pp. 1041-1048, July 1973, doi: https://doi.org/10.1007/BF00756636.

[21] M.P. Borom, A.M. Turkalo, R.H. Doremus, “Strength and microstructure in lithium disilicate glass-ceramics”, J. Amer. Ceram. Soc., vol. 58 no. 9-10, pp. 385-391, September 1975, doi: https://doi.org/10.1111/j.1151-2916.1975.tb19004.x.

[22] J.J. Mecholsky, "Fracture mechanics analysis of glass-ceramics", In: "Advances in Ceramics", Columbus, Ohio: The American Ceramic Society, 1982, 4, 261-276.

[23] G.H. Beall, "Glass-ceramics recent development and application", In: "Nucleation and Crystallization in Glasses and Liquids." Ceramic Transactions, Westerville, Ohio: The American Ceramic Society, 1993, 30, pp. 241-266.

[24] L.M. Echeverria, "New lithium disilicate glass-ceramic", Bol. Soc. Esp. Ceram. Vidrio, vol. 5, pp. 183-188, 1992.

[25] W. Höland, E. Apel, C. van’t Hoen, V. Rheinberger, "Studies of crystal phase formation in high-strength lithium disilicate glass-ceramics", J. Non-Cryst. Solids, vol. 352 no. 38-39, pp. 4041-4050, October 2006, doi: https://doi.org/10.1016/j.jnoncrysol.2006.06.039.

[26] E. Apel, C. van’t Hoen, V. Rheinberger, W. Höland, "Influence of ZrO_2 on the crystallization and properties of lithium disilicate glass-ceramic derived from multi-component system", J. Eur. Ceram. Soc., vol. 27 no. 2-3, pp. 1571-1577, 2007, doi: https://doi.org/10.1016/j.jeurceramsoc.2006.04.103.

[27] Q. Fu, G.H. Beall, C.M. Smith, "Nature-inspired design of strong, tough glass-ceramics", MRS Bulletin, vol. 42, pp. 220-225, March 2017, doi: https://doi.org/10.1557/mrs.2017.31.

[28] M.O.C. Villas-Boas, F.C. Serbena, V.O. Soares, I. Mathias, E.D. Zanotto, “Residual stress-effect on the fracture toughness of lithium disilicate glass-ceramics”, J. Amer. Ceram. Soc., vol. 103 no. 1, pp. 465-479, January 2020, doi: https://doi.org/10.1111/jace.16664.

[29] W. Liao, M. Rampf, M. Dittmer, C. Coperet, W. Höland, "Nucleation and Crystal Formation in Lithium Disilicate-Apatite Glass-Ceramic from Combined Use of X-Ray Diffraction, Solid-State NMR, and Microscopy", Helvetica Chimica Acta, 102, e1800210, December 2018, doi: https://doi.org/10.1002/hlca.201800210.

[30] D. Ehrt, M. Leister, A. Matthai, “Polyvalent elements iron, tin and titanium in silicate, phosphate and fluoride glasses and melts” Phys. Chem. Glasses, vol. 42 no. 3, pp. 231-239, June 2001.

[31] D. Ehrt, “Redox behaviour of Sn^{4+}/Sn^{2+} in alkali free aluminosilicate glasses and melts”, Phys. Chem. Glasses: Eur. J. Glass Sci. Technol. B, vol. 49 no. 2, pp. 68-72, April 2008.

[32] F. D. Doenitz, G. Welsch, W. Vogel, "Zur Rolle des Zinns in Glaskeramiken des Systems MgO-Al_2O_3-SiO_2", Silikattechnik, 35, Heft 2, 1984.

[33] J. Zhang, J. Huang, Y. Yu, Z. Zhang, H. Bai, Y. Huang, “Effect of substitution of ZrO_2 by SnO_2 on crystallization and properties of environment-friendly Li_2O–Al_2O_3–SiO_2 system (LAS) glass-ceramics”, Ceramics International, vol. 48 no. 15, pp. 21355–21361, August 2022, doi: https://doi.org/10.1016/j.ceramint.2022.04.101.

[34] M. Dressler, B. Rüdinger, J. Deubener, “Crystallization kinetics in a lithium alumosilicate glass using SnO_2 and ZrO_2 additives”, J. Non. Cryst. Sol., vol. 389, pp. 60-65, April 2014, doi: https://doi.org/10.1016/j.jnoncrysol.2014.02.008.

[35] C. Thieme, K. Thieme, M. Kracker, T. Höche, C. Rüssel, ”Role of Tin Oxide as a Nucleating Agent with Low Solubility in BaO−SrO−ZnO−SiO_2 Glasses Studied by Electron and

X-ray Microscopy”, Cryst. Growth Des., vol. 19 no.3, pp. 1815−1824, January 2019, doi: https://doi.org/10.1021/acs.cgd.8b01790.

[36] E. C. Ziemath, B. Z. Saggioro, J. S. Fossa, “Physical properties of silicate glasses doped with SnO_2”, J. Non. Cryst. Sol., vol. 351, no. 52-54, pp. 3870-3878, December 2005, doi: https://doi.org/10.1016/j.jnoncrysol.2005.10.016.

[37] J. Zhao, Y. Wang, J. Kang, Y. Qu, G. A. Khater, S. Li, Q. Shi, Y. Yue, “Effect of SnO_2 on the structure and chemical durability of the glass prepared by red mud”, J. Non. Cryst. Sol., vol. 509, pp. 54-59, April 2019, doi: https://doi.org/10.1016/j.jnoncrysol.2019.01.029.